

# Isotopic Effects in $XH_3$ ( $C_{3v}$ ) Molecules: The Lowest Vibrational Bands of $PH_2D$ Reinvestigated

O. N. Ulenikov,\* E. S. Bekhtereva,\* G. A. Onopenko,\* E. A. Sinitsin,\* H. Bürger,† and W. Jerzembek†

\*Laboratory of Molecular Spectroscopy, Physics Department, Tomsk State University, Tomsk 634050, Russia; and †Anorganische Chemie, Fachbereich 9, Universität–Gesamthochschule, D-42097 Wuppertal, Germany

E-mail: Ulenikov@phys.tsu.ru

Received March 27, 2001; in revised form June 1, 2001

We have derived, for  ${}^M X^m Y_3$  ( $C_{3v}$  symmetry) molecules which satisfy the conditions of a small ratio of atomic masses  $m_H/m_X$  and of equilibrium angles  $Y-X-Y$  close to  $\pi/2$ , simple isotopic relations for rotation–vibration parameters  $\alpha_\lambda^\beta$  for the case where one light atom  $Y$  ( $=H$ ) is replaced by a heavier one ( $=D$ ). The usefulness and predictive power of such relations for the assignment and in the fit were tested by analyzing novel high resolution Fourier transform spectra of the  $PH_2D$  molecule. The region of the three lowest-lying vibrational–rotational bands  $\nu_4$ ,  $\nu_6$ , and  $\nu_3$  was studied. The accurate analysis was made possible with the help of recently obtained (O. N. Ulenikov, H. Bürger, W. Jerzembek, G. A. Onopenko, E. S. Bekhtereva, and O. L. Petrunina, *J. Mol. Struct.*, in press) precise rotational energies of the ground vibrational state of  $PH_2D$ . This improvement, in conjunction with better resolution and higher sensitivity, enabled us to assign transitions with higher values of quantum numbers  $J$  and  $K_c$  and to obtain more accurate rotation–vibration energies of upper states than previously. These energies, fitted with a Watson-type Hamiltonian in  $A$  reduction and  $III'$  representation, lead to a physically meaningful set of spectroscopic parameters which reproduce the experimental energies with a precision close to experimental uncertainty. Agreement between predicted and fitted Coriolis and vibrational constants is noted; apparent limitations are caused by significant deviation of  $PH_3$  and  $PH_2D$  from the idealized local mode case model. © 2001 Academic Press

**Key Words:** vibration–rotation spectra;  $PH_2D$  molecule; spectroscopic parameters.

## 1. INTRODUCTION

In recent contributions (1, 2) we derived and discussed sets of simple isotopic relations which connect spectroscopic parameters of near-local-mode molecules  $XH_2$  ( $C_{2v}$ ) and their substituted  $XD_2$  ( $C_{2v}$ ) and  $XHD$  ( $C_i$ ) species. The predictions derived by relations show impressively high predictive power when compared with the results of analysis of experimental vibration–rotation spectra of the  $D_2Se$  and  $HSe$  molecules. In continuation of this work, the present contribution is devoted to the analysis of the analogous problem relating  $XH_3$  ( $C_{3v}$ ) and  $XH_2D$  ( $C_s$ ) molecules. Here  $XH_3$  is an axially symmetric, 4-atomic molecule which we call a “near-local-mode molecule” if it satisfies the conditions

- (a) the ratio of atomic masses  $m_H/M_X$  is small;
- (b) the equilibrium angle  $H-X-H$  is close to  $\pi/2$ ;
- (c) the  $X-H$  stretching frequencies are very close to each other and considerably larger than the bending frequencies.

In the present study, the  $PH_2D$  molecule is used as a test case for the derived theoretical results. The study of high-resolution vibration–rotation spectra of the  $PH_3$  molecule and its isotopic species is a project of general interest. On the one hand, phosphine plays an important role in astrophysics and planetology

(see, e.g., Refs. (3–5), and references therein), which generates large interest in laboratory spectroscopic investigations of this molecule. On the other hand, the phosphine molecule is one of the lightest and simplest symmetric top molecules. Hence spectroscopic effects and peculiarities inherent to symmetric tops should be particularly pronounced in its spectra. Moreover, in our opinion  $PH_3$  and its different isotopic species can be considered as test cases to examine the validity and accuracy of different theoretical approaches, in particular those commonly used for modeling isotopic substitution effects in  $XH_3$  molecules which satisfy the above mentioned conditions (a)–(c).

Extensive studies of  $PH_3$  spectra have been performed in the infrared region (see (6–8) and references cited therein). To the contrary, there are only two contributions devoted to the analysis of infrared spectra of the  $PH_2D$  species: the bands  $\nu_2(a')$ ,  $\nu_3(a')$ ,  $\nu_4(a')$ , and  $\nu_6(a'')$  [ $\nu_{3a}$ ,  $\nu_{4a}$ ,  $\nu_2$ , and  $\nu_{4b}$  in the notation of Refs. (9, 10)] have been investigated, and an interaction model involving Coriolis resonances between  $\nu_3$ ,  $\nu_4$  and  $\nu_6$  has been established (10). As was mentioned in our earlier work (11), we have recorded high-resolution spectra of the  $PH_2D$  molecule in the wide spectral region from 20 to 5000  $cm^{-1}$ . Having analyzed the far infrared, pure rotational part of the recorded spectrum, we felt that a reanalysis of the lowest vibrational bands due to the bending modes  $\nu_3$ ,  $\nu_4$ , and  $\nu_6$  would be appropriate in spite of the fine previous work (10) for several reasons.

First, the ground state rotational energies obtained in (11) are significantly more accurate than those obtained in Refs. (9, 10), because of the large body of more accurate data, and this is of relevance also for the excited states.

Second, the higher resolution ( $2.3 \times 10^{-3} \text{ cm}^{-1}$ , 1/maximum optical path difference) than in (9, 10) ( $5 \times 10^{-3} \text{ cm}^{-1}$ ) and the higher signal:noise ratio of our experimental data in comparison with those of Refs. (9, 10) enabled us to assign weaker lines. This gave us the possibility of observing transitions with higher values of the quantum numbers  $J$  and  $K_c$  ( $K_a$  in the notation of Refs. (9) and (10)). Thereof, we were able to deduce more precise and extensive information on the rotational structure and spectroscopic parameters of the states (001000), (000100), and (000001) in the notation ( $\nu_1 \nu_2 \nu_3 \nu_4 \nu_5 \nu_6$ ).

Third, and most importantly, we use the present data on PH<sub>2</sub>D as a test case for the relations deduced for isotopic substitution  $\text{XH}_3 \rightarrow \text{XH}_2\text{D}$ . This will be elaborated in Section 2 of the present contribution.

Sections 3 and 4 are devoted to a short description of the experimental details and the used Hamiltonian model. The assignment of experimental transitions and the results of the reanalysis will be discussed in Section 5.

## 2. ISOTOPIC SUBSTITUTION $\text{XH}_3 \rightarrow \text{XH}_2\text{D}$ IN AN $\text{XH}_3$ MOLECULE WITH $C_{3v}$ SYMMETRY

From a general physical point it is obvious that a number of relations must exist between different isotopic species of molecules when they physically only differ from each other by the atomic masses. As was discussed in Ref. (12), the possibility of deriving such isotopic relations is mathematically based on the fact that exact connections exist between transformation coefficients  $l_{N\alpha\mu}$  and  $l'_{K\gamma\lambda}$  of a “mother” and a “daughter” species, respectively:

$$l'_{N\beta\lambda} = \sum_{\alpha\mu} \mathcal{K}_{\alpha\beta}^e (m_N/m'_N)^{1/2} l_{N\alpha\mu} \beta_{\lambda\mu}. \quad [1]$$

Here  $m_N$  and  $m'_N$  are the masses of the  $N$ th atom before and after isotopic substitution, respectively. The coefficients  $\beta_{\lambda\mu}$  are the elements of the matrix which is inverse to the matrix  $\alpha_{\lambda\mu}$ . The matrix  $\alpha_{\lambda\mu}$  performs the transformation from the normal vibrational coordinates of a “mother” molecule to those of a “daughter” species. The matrix elements  $\alpha_{\lambda\mu}$  are determined by (see, for details, Ref. (12))

$$\sum_{\nu} \alpha_{\lambda\nu} \alpha_{\mu\nu} = A_{\lambda\mu} = \sum_{N\alpha} \frac{m_N}{m'_N} l_{N\alpha\lambda} l_{N\alpha\mu}, \quad [2]$$

$$\sum_{\nu} A_{\lambda\nu} W_{\nu} \alpha_{\nu\mu} = \alpha_{\lambda\mu} W'_{\mu} \quad [3]$$

and lead to the secular equation

$$\det\{\mathbf{AW} - \mathbf{W}'\} = 0,$$

where  $\mathbf{A}$  is the matrix with the elements  $A_{\lambda\nu}$ ;  $\mathbf{W}$  and  $\mathbf{W}'$  are the diagonal matrices with the elements  $W_{\lambda\nu} = \omega_{\lambda}^2 \delta_{\lambda\nu}$  and  $W'_{\lambda\nu} = \omega'^2_{\lambda} \delta_{\lambda\nu}$ , respectively; and  $\omega_{\lambda}$  and  $\omega'_{\lambda}$  are the harmonic frequencies of a parent and substituted species, respectively.

The parameters  $\mathcal{K}_{\alpha\beta}^e$  can be found from the normalization conditions

$$\sum_{\alpha} \mathcal{K}_{\alpha\beta}^e \mathcal{K}_{\alpha\gamma}^e = \sum_{\alpha} \mathcal{K}_{\beta\alpha}^e \mathcal{K}_{\gamma\alpha}^e = \delta_{\beta\gamma} \quad [4]$$

and

$$\sum_{\beta} J_{\alpha\beta}^e \mathcal{K}_{\beta\gamma}^e = I'_{\gamma\gamma} \mathcal{K}_{\alpha\gamma}^e, \quad [5]$$

where  $I'_{\gamma\gamma}$  denotes the equilibrium moments of inertia of the substituted molecule. The terms  $J_{\alpha\beta}^e$  are determined by the formulae

$$J_{\alpha\beta}^e = \sum_{\gamma\delta\kappa} \varepsilon_{\alpha\gamma\kappa} \varepsilon_{\beta\delta\kappa} j_{\gamma\delta}^e \quad [6]$$

and

$$j_{\gamma\delta}^e = j_{\delta\gamma}^e = \sum_N m'_N r_{N\gamma}^e r_{N\delta}^e - \frac{\sum_K m'_K r_{K\gamma}^e \sum_L m'_L r_{L\delta}^e}{\sum_N m'_N}. \quad [7]$$

Here  $r_{N\alpha}^e$  are the Cartesian coordinates defining the equilibrium positions of the nuclei of the “mother” species in the molecule-fixed axis system. The values  $\mathcal{K}_{\alpha\gamma}^e$  can be also considered as the eigenvectors of the “inertia tensor”  $J_{\alpha\beta}^e$  with the eigenvalues  $I'_{\gamma\gamma}$ .

Further use of Eq. [1] in customary formulae of conventional vibration-rotation theory (see, e.g., (13, 14)) allows one, in principle, to establish connections with other spectroscopic parameters of different isotopic species. It should be mentioned, however, that Eq. [1], in the general case, is very complicated, and the values occurring in the right-hand side of Eq. [1] may be determinable only numerically and in consequence, isotopic relations may also be obtained only numerically. The main reason for this limitation is the complicated form of the transformation coefficients  $l_{N\alpha\mu}$  of the “mother” species.

As was shown (15), the transformation coefficients  $l_{N\alpha\mu}$  of the “mother” species have a very simple form, which for convenience is reproduced again in Table 1, when an  $\text{XH}_3$  molecule (with  $C_{3v}$  symmetry) possesses some special properties, namely

- the ratio of the atomic masses  $m_H/m_X$  is small;
- the equilibrium angles H–X–H are close to  $\pi/2$ ;
- there are no interactions between stretching and bending motions in the quadratic part of intramolecular potential function, i.e., parameters  $f_{rr}$ ,  $f_{rr'}$ ,  $f_{\alpha\alpha}$ , and  $f_{\alpha\beta}$  are nonzero, but  $f_{r\alpha} = f_{r\beta} = 0$ .

In case these approximations are valid one can expect that analogous simple relations can also be derived for a “daughter”

**TABLE 1**  
**Values of  $l_{N\alpha\lambda}$  Parameters of an  $XY_3$  Molecule**  
**in the Local Mode Limit<sup>a</sup>**

$N$	$\alpha$	$\lambda$	$s$	$l_{N\alpha\lambda}$	$N$	$\alpha$	$\lambda$	$s$	$l_{N\alpha\lambda}$
1	x	1		$\sqrt{2}/3$	1	x	2		1/3
2	x	1		$-\sqrt{2}/6$	2	x	2		-1/6
3	x	1		$-\sqrt{2}/6$	3	x	2		-1/6
1	y	1		0	1	y	2		0
2	y	1		$-1/\sqrt{6}$	2	y	2		$-1/2\sqrt{3}$
3	y	1		$1/\sqrt{6}$	3	y	2		$1/2\sqrt{3}$
1	z	1		-1/3	1	z	2		$\sqrt{2}/3$
2	z	1		-1/3	2	z	2		$\sqrt{2}/3$
3	z	1		-1/3	3	z	2		$\sqrt{2}/3$
1	x	3	1	2/3	1	x	4	1	$1/3\sqrt{2}$
2	x	3	1	1/6	2	x	4	1	$-\sqrt{2}/3$
3	x	3	1	1/6	3	x	4	1	$-\sqrt{2}/3$
1	y	3	1	0	1	y	4	1	0
2	y	3	1	$1/2\sqrt{3}$	2	y	4	1	$1/\sqrt{6}$
3	y	3	1	$-1/2\sqrt{3}$	3	y	4	1	$-1/\sqrt{6}$
1	z	3	1	$-\sqrt{2}/3$	1	z	4	1	1/3
2	z	3	1	$1/3\sqrt{2}$	2	z	4	1	-1/6
3	z	3	1	$1/3\sqrt{2}$	3	z	4	1	-1/6
1	x	3	2	0	1	x	4	2	0
2	x	3	2	$1/2\sqrt{3}$	2	x	4	2	$1/\sqrt{6}$
3	x	3	2	$-1/2\sqrt{3}$	3	x	4	2	$-1/\sqrt{6}$
1	y	3	2	0	1	y	4	2	$-1/\sqrt{2}$
2	y	3	2	1/2	2	y	4	2	0
3	y	3	2	1/2	3	y	4	2	0
1	z	3	2	0	1	z	4	2	0
2	z	3	2	$1/\sqrt{6}$	2	z	4	2	$-1/2\sqrt{3}$
3	z	3	2	$-1/\sqrt{6}$	3	z	4	2	$1/2\sqrt{3}$

<sup>a</sup> All parameters  $l_{4\alpha\lambda s}$  are equal to zero.

species on the basis of the general expression [1]. Here we consider the case in which only one H atom is substituted by a D atom (atom 1 in Fig. 1). In this case, making use of the conditions (a)–(c) as defined above in the general formulae [2]–[7] yields the following simple nonzero values of the  $\mathcal{K}_{\alpha\beta}^e$  and  $\beta_{\lambda\mu}$

coefficients:

$$\begin{aligned} \mathcal{K}_{xx}^e &= 1/\sqrt{3} & \mathcal{K}_{xz}^e &= -\sqrt{2}/3 & \mathcal{K}_{zx}^e &= \sqrt{2}/3 \\ \mathcal{K}_{zz}^e &= 1/\sqrt{3} & \mathcal{K}_{yy}^e &= 1; \\ \beta_{11} &= \sqrt{2}/3 & \beta_{21} &= \sqrt{2}/3 & \beta_{13_1} &= -1/\sqrt{3} & \beta_{23_1} &= 2/\sqrt{3} \\ \beta_{32} &= 1/\sqrt{3} & \beta_{42} &= 2\sqrt{2}/3 & \beta_{34_1} &= -\sqrt{2}/3 & \beta_{44_1} &= 2/3 \\ \beta_{53_2} &= 1 & \beta_{64_2} &= 2/\sqrt{3}. \end{aligned} \quad [8]$$

From the above discussion it is clear that the  $\mathcal{K}_{\alpha\gamma}^e$  coefficients can be also considered as the elements of the matrix which describe a rotation of the molecular fixed coordinate axis under isotopic substitution  $XH_3 \rightarrow XH_2D$ . In this case, it may be interesting to discuss the accuracy of the used local mode approximation. This can be made, for example, by comparing the value of the angle  $\chi$  under rotation of the intramolecular coordinate axis both in the local mode model, and in the “realistic” case (i.e.,  $m_H/M \neq 0$ ;  $\alpha_e \neq 90^\circ$ ). In this present case, as can be seen from the above discussion, the rotation is performed about the y axis. Figure 2 shows the dependence of the value of the angle  $\chi$  on the values of the mass  $M$  ( $m_H = 1$ ) and the equilibrium interbond angle  $\alpha_e$ . Here, point A corresponds to the local mode model ( $m_H/M$  close to zero;  $\alpha_e = 90^\circ$ ); point B corresponds the actual  $PH_3$  molecule ( $m_H/M_P = 1/31$ ;  $\alpha_e = 93.45^\circ$  [16]). As the calculations show, the differences in the  $\mathcal{K}_{\alpha\gamma}^e$  values between the local mode model and the “realistic” one may achieve values of 20–25% for the substitution  $PH_3 \rightarrow PH_2D$ . At the same time, Fig. 2 shows that the values of such differences are decreasing rapidly with increasing mass  $M$  and/or decreasing value of ( $\alpha_e - 90^\circ$ ). For example, for the  $AsH_3 \rightarrow AsH_2D$  substitution, the above mentioned differences in the  $\mathcal{K}_{\alpha\gamma}^e$  values are as small as 4–6%.

Using relations [8], [9] and the values of the transformation coefficients  $l_{N\alpha\mu}$  of the “mother” molecule  $XH_3$  as reported in Table 1 in the general formula [1], one can obtain without difficulties very simple relations for the  $l'_{K\beta\lambda}$  transformation

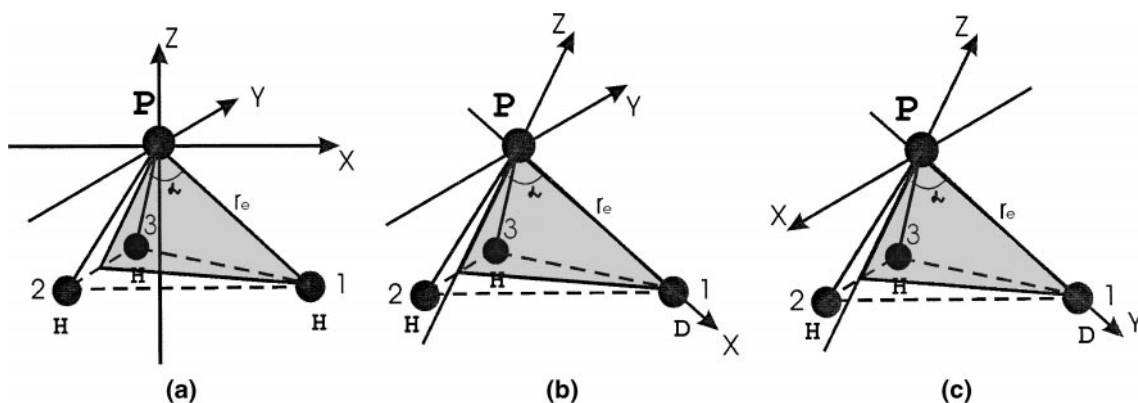


**FIG. 1.** (a) Orientation of the coordinate axis in the “mother”  $XH_3$  molecule. (b) Orientation of the coordinate axis in the “daughter”  $XH_2D$  molecule after rotation. (c) Orientation of the coordinate axis which corresponds to the  $III'$  representation in the  $XH_2D$  molecule.

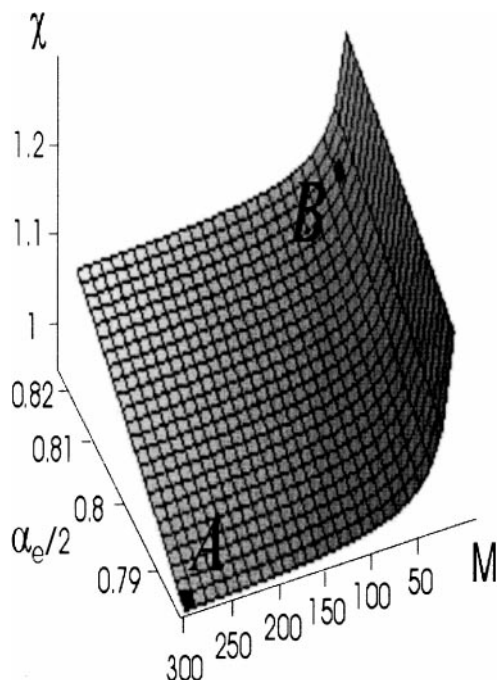


**FIG. 2.** The dependence of the value of the angle  $\chi$  (in radians) on the value of the mass  $M$  (in  $u$ ) of the  $X$  nucleus and the value of the equilibrium interbond angle  $\alpha_e$  (in radians) is shown. Here the angle  $\chi$  is the angle of rotation of the molecular fixed coordinate axis under  $XH_3 \rightarrow XH_2D$  substitution. Point  $A$  corresponds to the local mode model ( $m_H/M$  close to zero;  $\alpha_e = 90^\circ$ ); point  $B$  corresponds to the  $PH_3$  molecule ( $m_H/M_P = 1/31$ ;  $\alpha_e = 93.45^\circ$  (13)).

coefficients for the  $XH_2D$  species. It should be mentioned that the relations Eq. [8] determine the rotation of the molecular coordinate axis from the configuration shown in Fig. 1a to the configuration illustrated in Fig. 1b. At the same time, as was discussed in (11), the coordinate axes for the  $PH_2D$  molecule should be oriented as shown in Fig. 1c. This means that the indices  $\beta$  appearing in the transformation coefficients  $l'_{K\beta\lambda}$  determined as described above should be relabelled in accordance with the axis in Fig. 1c. The coefficients  $l'_{K\alpha\lambda}$  eventually obtained are presented in Table 2.

These coefficients are the basis to derive simple expressions for different rovibrational parameters, such as Coriolis coefficients  $\zeta_{\lambda,\mu}^{\alpha}$  and rotation–vibration coefficients  $a_{\lambda}^{\alpha\beta}$ . These Coriolis coefficients  $\zeta_{\lambda,\mu}^{\alpha}$  and ro-vibrational parameters  $a_{\lambda}^{\alpha\beta}$ , respectively, are given in

$$\begin{aligned} \zeta_{1,4}^{lx} &= -\zeta_{2,4}^{lx} = -\zeta_{3,4}^{lx} = \zeta_{5,6}^{lx} = -\zeta_{1,6}^{lz} = \zeta_{2,6}^{lz} = -\zeta_{3,6}^{lz} \\ &= \zeta_{4,5}^{lz} = -1/\sqrt{3}, \quad \zeta_{3,5}^{ly} = -1, \quad \zeta_{4,6}^{ly} = 1/3; \end{aligned} \quad [10]$$

$$\begin{aligned} a_1^{xx} &= a_1^{yy}/2 = a_1^{zz} = a_2^{xx}/2 = a_2^{zz}/2 = -a_3^{xx} = a_3^{zz} \\ &= -a_5^{xz} = -a_5^{zx} = \sqrt{2m_H r_e^2}, \end{aligned}$$

$$a_4^{yz} = a_4^{zy} = a_6^{xy} = a_6^{yx} = -2\sqrt{2m_H r_e^2}/\sqrt{3}. \quad [11]$$

In turn, we have used Eqs. [10] and [11] to calculate rotational–vibrational spectroscopic parameters  $\alpha_{\lambda}^{\alpha\beta}$  of  $PH_2D$ . In this case, the same above-mentioned approximation for the intramolecular potential function as for the “mother” molecule  $PH_3$  (15) was used, too, for  $PH_2D$ . We have derived simple isotopic relations for the rotation–vibration parameters of the bending modes:

$$\begin{aligned} \alpha_3^{lx} &= \alpha_3^{lz} = \frac{8}{9} \frac{B_e^2}{\theta\omega} (\theta^2 - 1 + 2c); \\ \alpha_4^{lx} &= \alpha_6^{lz} = \frac{4}{27\sqrt{3}} \frac{B_e^2}{\theta\omega} (42\theta^2 - 23 + 9c/2) \\ &\quad + \frac{16}{27\sqrt{3}} \frac{B_e^2}{\theta\omega} \left( \frac{4+9\theta^2}{4-3\theta^2} + \frac{2+9\theta^2}{2-3\theta^2} \right); \\ \alpha_6^{lx} &= \alpha_4^{lz} = \frac{28}{9\sqrt{3}} \frac{B_e^2}{\theta\omega} (2\theta^2 - 1 + 3c/14) \\ &\quad + \frac{16}{27\sqrt{3}} \frac{B_e^2}{\theta\omega} \left( \frac{4+9\theta^2}{4-3\theta^2} \right); \\ \alpha_3^{ly} &= 4 \frac{B_e^2}{\theta\omega} \left( \frac{3-\theta^2}{1-\theta^2} \right) \theta^2; \\ \alpha_4^{ly} &= \alpha_6^{ly} = \frac{4}{3\sqrt{3}} \frac{B_e^2}{\theta\omega} (3\theta^2 - 4 + 9c/4); \end{aligned} \quad [12]$$

Column 2 of Table 3 reports the calculated values for the bending vibrations  $\nu_3$ ,  $\nu_4$ , and  $\nu_6$ . The Coriolis interaction parameters  $A\zeta$ ,  $B\zeta$ , and  $C\zeta$  were calculated using the relations of Eq. [10] and the rotational constants  $A$ ,  $B$ , and  $C$  from Ref. (11). The  $B_e$  value was taken as  $B_e = h/(8\pi^2 c)(2m_H r_e^2)^{-1} = 4.2276 \text{ cm}^{-1}$ , with  $r_e = 1.412 \text{ \AA}$  taken from Ref. (17); the frequency  $\omega$  is  $(\omega_1 + \omega_3)/2 = 2324 \text{ cm}^{-1}$ . The empirical parameter  $\theta = (\theta_1 + \theta_2)/2 = 0.444 \text{ cm}^{-1}$  was estimated from the three quartic centrifugal

**TABLE 2**  
Values of Nonzero  $l_{N\alpha\lambda}$  Parameters of an  $XH_2D$  Molecule in the Local Model Limit<sup>a</sup>

$N$	$\alpha$	$\lambda$	$l_{N\alpha\lambda}$	$N$	$\alpha$	$\lambda$	$l_{N\alpha\lambda}$
2	$x$	1	1/2	2	$y$	4	$-1/\sqrt{3}$
3	$x$	1	-1/2	3	$y$	4	$-1/\sqrt{3}$
2	$z$	1	-1/2	1	$z$	4	$1/\sqrt{3}$
3	$z$	1	-1/2	2	$x$	5	-1/2
1	$y$	2	1	3	$x$	5	-1/2
2	$x$	3	1/2	2	$z$	5	1/2
3	$x$	3	-1/2	3	$z$	5	-1/2
2	$z$	3	1/2	1	$x$	6	$1/\sqrt{3}$
3	$z$	3	1/2	2	$y$	6	$1/\sqrt{3}$
				3	$y$	6	$-1/\sqrt{3}$

<sup>a</sup>All parameters  $l_{4\alpha\lambda}$  are equal to zero.

**TABLE 3**  
**Some Coriolis Interactions and Vibration-Rotation Parameters of the PH<sub>2</sub>D Molecule (in cm<sup>-1</sup>)**

Parameter	Value <sup>a)</sup>	Value <sup>b)</sup>
1	2	3
$B\zeta_{43}^x$	-1.72	-2.07
$C\zeta_{46}^x$	1.45	1.59
$A\zeta_{36}^x$	1.60	1.52
$\alpha_3^x$	-0.0006	-0.0011
$\alpha_3^y$	0.0477	0.0479
$\alpha_3^z$	-0.0006	0.0051
$\alpha_4^x$	0.0066	0.0044
$\alpha_4^y$	-0.0340	-0.0317
$\alpha_4^z$	-0.0063	-0.0076
$\alpha_6^x$	-0.0063	-0.0089
$\alpha_6^y$	-0.0340	-0.0450
$\alpha_6^z$	0.0066	0.0113

<sup>a</sup> Predicted on the basis of derived isotopic relations.

<sup>b</sup> Obtained from the fit of experimental data.

distortion coefficients of the PH<sub>3</sub> molecule in the ground vibrational state, Ref. (8), with the formulae

$$D_J = \frac{B_e^3}{3\omega^2}(9 + \theta_2^{-2} + 2\theta_4^{-2}), \quad D_{JK} = \frac{2B_e^3}{\omega^2}(1 - \theta_2^{-2}),$$

$$D_K = \frac{B_e^3}{3\omega^2}(-7 + 9\theta_2^{-2} - 2\theta_4^{-2}), \quad [13]$$

taken from Ref. (15). Parameter  $c$  in Eq. [12] can be determined, on the one hand, from an experimental value of one of the  $\alpha_\lambda^\beta$  rotation-vibration constants of the “mother” molecule PH<sub>3</sub> or, on the other hand, can be taken as an empirical parameter of the PH<sub>2</sub>D molecule. In the present analysis it was set to 0.38.<sup>1</sup>

The parameters given in column 2 of Table 3 were used as the starting values for fitting the experimental rovibrational energies of the (001000), (000100), and (000001) vibrational states of the PH<sub>2</sub>D molecule.

### 3. EXPERIMENTAL SECTION

The synthesis of phosphine enriched to 60% PHD<sub>2</sub>, 25% PH<sub>2</sub>D, 10% PD<sub>3</sub>, and 5% PH<sub>3</sub> (sample A) has been described (11). Moreover, a sample composed of 5% PH<sub>2</sub>D, 10% PHD<sub>2</sub>, and 85% PD<sub>3</sub> (sample B) was available for comparison and iden-

<sup>1</sup> In the first step of the analysis, values of the rotational parameters were roughly estimated from the fit of the energy levels with the quantum number  $J = 0$  and 1. The  $\alpha_\lambda^\beta$  parameters obtained from just that fit were used to estimate the coefficient of the  $c$  value.

tification of lines belonging to other isotopomers than PH<sub>2</sub>D by means of relative intensities of lines.

Spectra were recorded at room temperature with a Bruker 120 HR interferometer adjusted to a resolution of  $2.3 \times 10^{-3}$  cm<sup>-1</sup> (1/maximum optical path difference) in the region 600–1160 cm<sup>-1</sup>. A Globar source, a KBr/Ge beam splitter, and an MCT 600 detector were employed, and a 8.5 μm low-pass filter was inserted. A 28-cm glass cell fitted with KBr windows was used, with pressures ranging from 100 to 550 Pa. Between 150 and 400 scans were collected for the different spectra. Calibration was done with CO<sub>2</sub> lines (18); wavenumber precision of unblended, medium intensity lines is about  $1 \times 10^{-4}$  cm<sup>-1</sup>. It was ensured that wavenumbers of different spectra were compatible with each other within one precision interval. Two portions of the spectrum are illustrated in Figs. 3 and 4, and some assignments are given.

## 4. HAMILTONIAN MODEL AND WAVE FUNCTIONS

### 4.1. Rovibrational Hamiltonian

As was discussed in (11), the PH<sub>2</sub>D molecule is an asymmetric top very close to the prolate symmetric top limit, and III' representation of the rotational Watson-type Hamiltonian in  $A$  reduction is very efficient. This is taken as

$$H^{ii} = E^i + \left[ A^i - \frac{1}{2}(B^i + C^i) \right] J_z^2 + \frac{1}{2}(B^i + C^i) J^2$$

$$+ \frac{1}{2}(B^i - C^i) J_{xy}^2 - \Delta_K^i J_z^4 - \Delta_{JK}^i J_z^2 J^2$$

$$- \Delta_J^i J^4 - \delta_{JK}^i [J_z^2, J_{xy}^2] - 2\delta_J^i J^2 J_{xy}^2 + H_K^i J_z^6$$

$$+ H_{KJ}^i J_z^4 J^2 + H_{JK}^i J_z^2 J^4 + H_J^i J^6 + [J_{xy}^2, h_K^i J_z^4$$

$$+ h_{JK}^i J^2 J_z^2 + h_J^i J^4] + L_K^i J_z^8 + L_{KJ}^i J_z^6 J^2$$

$$+ L_{JK}^i J_z^4 J^4 + L_{KJJ}^i J_z^2 J^6 + L_J^i J^8 + [J_{xy}^2, l_K^i J_z^6$$

$$+ l_{KJ}^i J^2 J_z^4 + l_{JK}^i J^4 J_z^2 + l_J^i J^6] + \dots, \quad [14]$$

where the condition  $B_y > B_x > B_z$  is fulfilled,  $J_{xy}^2 = J_x^2 - J_y^2$ , and  $J^2 = J_x^2 + J_y^2 + J_z^2$ . The PH<sub>2</sub>D molecule has C<sub>s</sub> symmetry. Its three lowest vibrational bands,  $\nu_4$ ,  $\nu_6$ , and  $\nu_3$ , have A', A'', and A' symmetries, respectively, and interact strongly with each other. On this reason, a Hamiltonian was used which has the form

$$H^{v..r.} = \sum_{i,j} |i\rangle \langle j| H^{ij}, \quad [15]$$

where  $i = 4, 3, 6$ , and  $|4\rangle = (000100)$ ,  $|3\rangle = (001000)$ , and  $|6\rangle = (000001)$ . The diagonal parts  $H^{ii}$  have the form of Eq. [14]. Interactions between the states (000100) and (001000) on the one hand and the state (000001) on the other hand are described by the  $H^{i6}$  ( $i = 3$  or 4) operators

$$H^{i6} = H^{6i+} = H_{C_z}^{i6} + H_{C_y}^{i6}, \quad [16]$$

where

$$\begin{aligned}
 H_{C_z}^{i6} = & 2(A\zeta^z)^{i6}iJ_z + C_{zK}^{i6}iJ_z^3 + C_{zJ}^{i6}iJ_zJ^2 + C_{zKK}^{i6}iJ_z^5 \\
 & + C_{zJK}^{i6}iJ_z^3J^2 + C_{zJJ}^{i6}iJ_zJ^4 + C_{zKKK}^{i6}iJ_z^7 + \dots \\
 & + C_{xy}^{i6}[J_x, J_y]_+ + C_{xyK}^{i6}[[J_x, J_y]_+, J_z^2]_+ \\
 & + C_{xyJ}^{i6}[J_x, J_y]_+J^2 + C_{xyKK}^{i6}[[J_x, J_y]_+, J_z^4]_+ \\
 & + C_{xyJK}^{i6}[[J_x, J_y]_+, J_z^2J^2]_+ + C_{xyJJ}^{i6}[J_x, J_y]_+J^4 + \dots
 \end{aligned} \quad [17]$$

and

$$\begin{aligned}
 H_{C_y}^{i6} = & 2(B\zeta^y)^{i6}iJ_y + C_{yK}^{i6}[iJ_y, J_z^2]_+ + C_{yJ}^{i6}iJ_yJ^2 \\
 & + C_{yKK}^{i6}[iJ_y, J_z^4]_+ + C_{yJK}^{i6}[iJ_y, J_z^2J^2]_+ + C_{yJJ}^{i6}iJ_yJ^4 \\
 & + C_{yKKK}^{i6}[iJ_y, J_z^6]_+ + C_{yKKJ}^{i6}[iJ_y, J_z^4J^2]_+ \dots \\
 & + C_{xz}^{i6}[J_x, J_z]_+ + C_{xzK}^{i6}[[J_x, J_z]_+, J_z^2]_+ \\
 & + C_{0xzJ}^{i6}[J_x, J_z]_+J^2 + C_{xzKK}^{i6}[[J_x, J_z]_+, J_z^4]_+ \\
 & + C_{xzJK}^{i6}[[J_x, J_z]_+, J_z^2J^2]_+ + C_{xzJJ}^{i6}[J_x, J_z]_+J^4 + \dots
 \end{aligned} \quad [18]$$

In turn, the resonance interaction operator  $H^{43} = H^{34+}$  has the form

$$H^{43} = H_F^{43} + H_{C_x}^{43}, \quad [19]$$

where

$$\begin{aligned}
 H_F^{43} = & F^{43} + F_K^{43}J_z^2 + F_J^{43}J^2 + F_{KK}^{43}J_z^4 + F_{JK}^{43}J_z^2J^2 \\
 & + F_{JJ}^{43}J^4 + F_{KKK}^{43}J_z^6 + F_{KJJ}^{43}J_z^4J^2 + \dots \\
 & + F_{xy}^{43}J_{xy}^2 + F_{xyK}^{43}[J_{xy}^2, J_z^2]_+ + F_{xyJ}^{43}J_{xy}^2J^2 \\
 & + F_{xyKK}^{43}[J_{xy}^2, J_z^4]_+ + F_{xyJK}^{43}[J_{xy}^2, J_z^2J^2]_+ + \dots
 \end{aligned} \quad [20]$$

and

$$\begin{aligned}
 H_{C_x}^{43} = & 2(B\zeta^x)^{43}iJ_x + C_{xK}^{43}[iJ_x, J_z^2]_+ + C_{xJ}^{43}iJ_xJ^2 + \dots \\
 & + C_{yz}^{43}[J_y, J_z]_+ + C_{yzK}^{43}[[J_y, J_z]_+, J_z^2]_+ \\
 & + C_{yzJ}^{43}[J_y, J_z]_+J^2 + C_{yzKK}^{43}[[J_y, J_z]_+, J_z^4]_+ + \dots
 \end{aligned} \quad [21]$$

## 4.2. Rotational Wave Functions

In order to make the Hamiltonian matrix real, we have defined the wave functions as follows.

1. Symmetric rotational wave functions:

$$|JK, A'\rangle = \frac{i^J}{\sqrt{2}}\{|JK\rangle + (-1)^J|J - K\rangle\}$$

for  $K = 2, 4, 6, \dots$ ;

$$|JK, A'\rangle = \frac{i^{J+1}}{\sqrt{2}}\{|JK\rangle + (-1)^J|J - K\rangle\}$$

for  $K = 1, 3, 5, \dots$ ;

$$|J0, A'\rangle = i^J|J0\rangle$$

for  $J$  even.

2. Antisymmetric rotational wave functions:

$$|JK, A''\rangle = \frac{i^{J-1}}{\sqrt{2}}\{|JK\rangle - (-1)^J|J - K\rangle\}$$

for  $K = 2, 4, 6, \dots$ ;

$$|JK, A''\rangle = \frac{i^J}{\sqrt{2}}\{|JK\rangle - (-1)^J|J - K\rangle\}$$

for  $K = 1, 3, 5, \dots$ ;

$$|J0, A''\rangle = i(J-1)|J0\rangle$$

for  $J$  odd.

These functions were employed to set up the Hamiltonian matrix which was then used to fit the experimental data.

## 5. ASSIGNMENT AND RESULTS

While the  $\nu_3$  and  $\nu_4$  bands should be associated both with  $a$ - and  $c$ -type transitions, the  $\nu_6$  band is expected to reveal  $b$ -type structure. Indeed, all three types of transitions were observed in the bending triad band. In this case, the comparison of the ‘‘pilot’’ transitions,  $(J'K'_a = J'K'_c) \leftarrow (JK_a = JK_c)$ , ( $K'_c, K_c = 0$  and/or 1), for all three bands shows that the strengths of the  $a$ - and  $c$ -type transitions are not much different from each other in the  $\nu_3$  band. The same can be seen in the  $\nu_4$  band. At the same time, transitions of the  $\nu_3$  band are slightly weaker (about 15–20%) than corresponding transitions of the  $\nu_4$  band. As to the  $\nu_6$  band, the strengths of its ‘‘pilot’’ transitions are comparable with those of the corresponding ‘‘pilot’’ transitions of the  $\nu_4$  band.

Assignments were made using the ground state combination differences method, with ground state rotational energies taken from Ref. (11). For convenience, the ground state rotational parameters are included in Table 4 and given in column 2. The

**TABLE 4**  
**Rotational and Centrifugal Distortion Parameters for the Ground and the Bending Vibrational States of PH<sub>2</sub>D (in cm<sup>-1</sup>)<sup>a</sup>**

Parameter	(000000)	(001000)	(000100)	(000001)
1	2	3	4	5
$\nu$		1092.5573590(616)	892.9275476(600)	969.4810870(612)
$A$	2.78247196	2.7773997(996)	2.7900553(973)	2.7710934E(492)
$B$	2.98320620	2.9842695(550)	2.9787664(559)	2.99206545(621)
$C$	4.33657995	4.2886767(452)	4.3683207(459)	4.38163113(666)
$\Delta_K \times 10^4$	-0.873198	-0.88840(874)	-0.86470(920)	-0.88542(125)
$\Delta_{JK} \times 10^4$	0.639662	0.65733(754)	0.62208(198)	0.638184(456)
$\Delta_J \times 10^4$	0.600698	0.60487(116)	0.625370(112)	0.627852(348)
$\delta_K \times 10^4$	-0.777525	-0.777525	-0.777525	-0.777525
$\delta_J \times 10^4$	-0.075385	-0.075385	-0.075385	-0.075385
$H_K \times 10^8$	-0.90645	-0.90645	-0.90645	-0.90645
$H_{KJ} \times 10^8$	0.3123	0.3123	0.3123	0.3123
$H_{JK} \times 10^8$	0.3896	0.3896	0.3896	0.3896
$H_J \times 10^8$	0.30497	0.30497	0.30497	0.30497
$h_K \times 10^8$	0.25038	0.25038	0.25038	0.25038
$h_{JK} \times 10^8$	-0.92844	-0.92844	-0.92844	-0.92844
$h_J \times 10^8$	-0.08227	-0.08227	-0.08227	-0.08227
$L_K \times 10^{12}$	-6.524	-6.524	-6.524	-6.524
$L_{KKJ} \times 10^{12}$	14.354	14.354	14.354	14.354
$L_{JK} \times 10^{12}$	-9.298	-9.298	-9.298	-9.298
$L_{KJJ} \times 10^{12}$	1.9422	1.9422	1.9422	1.9422
$L_J \times 10^{12}$	-0.4997	-0.4997	-0.4997	-0.4997
$l_K \times 10^{12}$	-1.951	-1.951	-1.951	-1.951
$l_{KJ} \times 10^{12}$	1.702	1.702	1.702	1.702
$l_{JK} \times 10^{12}$	0.0	0.0	0.0	0.0
$l_J \times 10^{12}$	0.2114	0.2114	0.2114	0.2114

Note. Excited state parameters without confidence intervals given were fixed to the values of corresponding parameters of the ground vibrational state.

<sup>a</sup> Values in parentheses are  $1\sigma$  statistical confidence intervals.

present body of assignments comprised

$$\nu_4, J^{max} = 22, K_c^{max} = 17, n = 2560$$

$$\nu_3, J^{max} = 21, K_c^{max} = 15, n = 1590$$

$$\nu_6, J^{max} = 20, K_c^{max} = 14, n = 1350.$$

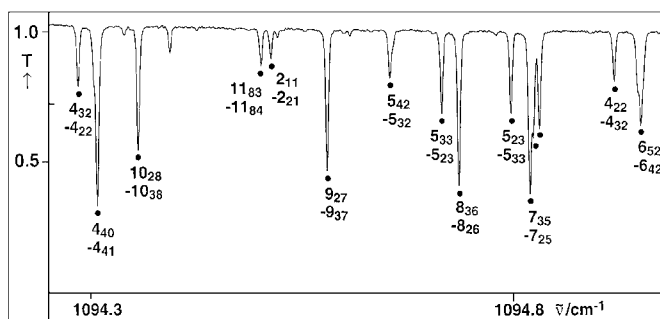


**FIG. 3.** Part of the PH<sub>2</sub>D spectrum in the region of the  $Q$ -branch of the  $\nu_3$  band. Lines of PH<sub>2</sub>D are denoted by a dot, and their  $J'_{K'_a K'_c} - J''_{K''_a K''_c}$  assignment is given. Unassigned lines belong to other isotopic species (PHD<sub>2</sub>, PD<sub>3</sub>, PH<sub>3</sub>).

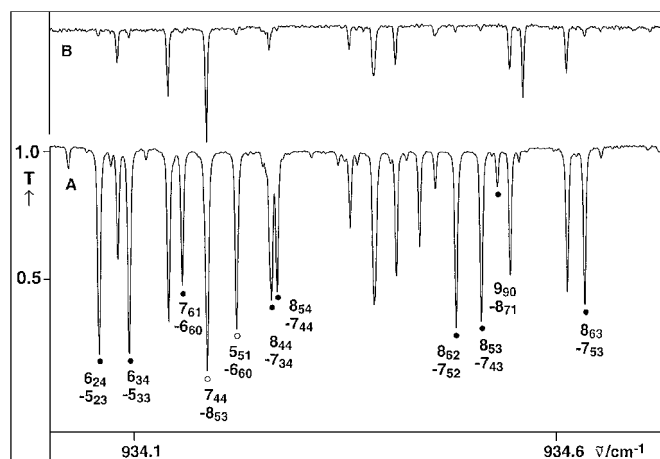


**FIG. 4.** Trace A: Spectrum of a mixture of PHD<sub>2</sub> and PH<sub>2</sub>D. Lines belonging to PH<sub>2</sub>D are assigned by full dots for the  $R$  branch of the  $\nu_4$  band and by open circles for the  $P$  branch of the  $\nu_6$  band. Unassigned lines belong to other isotopic species (PHD<sub>2</sub>, PD<sub>3</sub>, PH<sub>3</sub>). Trace B: Spectrum of a sample richer in PD<sub>3</sub> and poorer in PH<sub>2</sub>D and PH<sub>3</sub> shown for comparison.

**TABLE 5**  
**Some Assigned Transitions in the  $Q$ -Branch of the  $\nu_4$  Band of the PH<sub>2</sub>D Molecule**

$J'$	$K'_a$	$K'_c$	$J$	$K_a$	$K_c$	Line position <sup>a</sup> (cm <sup>-1</sup> )	Transm. (%)	$\nu_{exp}-\nu_{calc}$ 10 <sup>4</sup> cm <sup>-1</sup>	Line position <sup>b</sup> (cm <sup>-1</sup> )	$\nu_{exp}-\nu_{calc}$ 10 <sup>4</sup> cm <sup>-1</sup>
16	16	0	16	16	1	890.06237	68.5	1.5	890.0636	5.0
16	16	1	16	16	0	890.06759	69.6	0.2	890.0636	-48.0
5	3	3	5	2	3	890.16820	70.9	0.8	890.1698	8.0
15	15	0	15	15	1	890.18156	58.1	-0.7	890.1821	5.0
15	15	1	15	15	0	890.19100	54.5	-2.8	890.1907	-5.0
5	2	3	5	3	3	890.21240	73.1	0.9	890.2124	-7.0
4	1	4	4	0	4	890.27434	20.6	-0.3	890.2738	-13.0
14	14	0	14	14	1	890.29011	48.6	-2.0	890.2903	4.0
14	14	1	14	14	0	890.30714	47.8	-2.8	890.3074	4.0
17	4	13	16	1	15	890.37613	95.6	16.2		
13	13	0	13	13	1	890.38959	37.3	-2.5	890.3896	2.0
13	13	1	13	13	0	890.41938	37.3	-2.9	890.4192	0.0
3	3	1	3	2	1	890.44127	96.0	0.3		
12	12	0	12	12	1	890.48061	22.2	-2.0	890.4822	17.0
1	1	0	1	1	1	890.48350	47.5	1.2	890.4822	-1.0
15	11	5	15	11	4	890.48874	87.7	-3.5		
2	2	0	2	2	1	890.52282	30.9	-1.8	890.5237	0.0
12	12	1	12	12	0	890.53173	27.7	-2.4	890.5326	10.0
11	11	0	11	11	1	890.56247	20.3	-1.4	890.5628	3.0
3	3	0	3	3	1	890.57624	20.3	-1.0	890.5759	2.0
4	2	3	4	1	3	890.60884	62.1	-0.2	890.6102	5.0
7	5	2	7	6	2	890.61331	89.4	-1.6		
4	3	1	4	2	3	890.61999	61.3	0.0	890.6205	-2.0
4	4	0	4	4	1	890.63420	3.9	-9.0	890.6335	-11.0
11	11	1	11	11	0	890.64870	20.1	-1.4	890.6489	2.0
8	6	2	8	7	2	890.65597	91.2	-4.2		
6	4	2	6	5	2	890.68190	80.2	-1.7		
9	9	0	9	9	1	890.68888	1.5	-3.1	890.6879	-15.0
8	8	0	8	8	1	890.72577	1.3	-0.9	890.7251	-10.0
7	7	0	7	7	1	890.73889	8.7	1.7	890.7386	-3.0
8	7	2	8	7	1	890.77297	15.6	-1.0	890.7753	18.0
10	10	1	10	10	0	890.77591	12.9	0.4	890.7753	-6.0
10	8	3	10	8	2	890.79816	51.8	-0.5	890.7964	18.0
9	7	2	9	8	2	890.82761	94.9	-4.0		
5	3	2	5	4	2	890.83637	85.3	-0.2	890.8370	3.0
9	9	1	9	9	0	890.92029	10.7	1.2	890.9202	-2.0
3	1	3	3	0	3	890.94553	31.7	6.9	890.9456	0.0
3	0	3	3	1	3	890.94553	31.7	-9.3	890.9456	-15.0
4	2	2	4	3	2	891.04282	80.4	0.1	891.0427	-3.0
8	8	1	8	8	0	891.09107	8.4	2.0	891.0908	-4.0
3	2	2	3	1	2	891.12454	75.0	-0.9	891.1245	-3.0
10	8	2	10	9	2	891.13618	97.3	-1.0		
2	2	1	2	1	1	891.14401	91.4	-0.6	891.1440	4.0

<sup>a</sup> This work.<sup>b</sup> Ref. (10).

In accordance with the III' representation of the rotational Hamiltonian, rotational energies for given  $J$  increase with  $K_c$ .

The superiority of the present study to that of Ref.(10) can be underlined by some statistical data. Our  $J^{max}$  values, 22, 21, and 20, exceed those of (10), which were 20, 20, and 18, respectively, for  $\nu_4$ ,  $\nu_3$ , and  $\nu_6$ . The number of  $\nu_4$  and  $\nu_6$  band transitions, 2560 and 1350, respectively, is substantially larger than that in (10), 1579 and 1116. The 1590 transitions assigned for the  $\nu_3$  band seem to be less than the 1739 transitions assigned  $\leq 1235$  cm<sup>-1</sup> in (10). However, our spectrum was only exploited up to 1160 cm<sup>-1</sup> and the 1739 transitions should be compared with the 1357 assignments  $\leq 1160$  cm<sup>-1</sup> in Ref. (10).

Thanks to the significantly improved ground state energies, the higher precision of the present data, and the greater sensitivity of the actual spectrum, averaged experimental upper state energies were determined with an accuracy of  $0.23 \times 10^{-3}$  cm<sup>-1</sup>, which may be compared with the RMS of Ref. (10), ca.  $0.43 \times 10^{-3}$  cm<sup>-1</sup>. Two details of the spectra, with assignments of PH<sub>2</sub>D lines, are illustrated in Figs. 3 and 4. Table 5 reproducing a small part of the studied spectrum in the region of the  $\nu_4$  band center illustrates, on the one hand, that some weak lines not found in (10) were assigned in our study and, on the other hand, that line positions are reproduced 3–4 times more accurately. Averaged upper state energies obtained from different transitions reaching the same state are reported in Table 6, columns 2 ( $\nu_4$ ),







**TABLE 7**  
**Parameters of Resonance Interactions for the (000100), (001000), and (000001)**  
**Vibrational States of the PH<sub>2</sub>D Molecule (in cm<sup>-1</sup>)**

Coriolis-type interactions					
Parameter	Value	Parameter	Value	Parameter	Value
$(2B\zeta^x)^{1-2}$	-4.1498(898)	$C_{xK}^{1-2} \times 10^3$	-0.36994(662)	$C_{xJ}^{1-2} \times 10^3$	0.78534(892)
$C_{yz}^{1-2} \times 10$	-0.61276(226)	$C_{yJ}^{1-2} \times 10^4$	0.35560(786)	$C_{yzKK}^{1-2} \times 10^7$	0.4914(118)
$(2C\zeta^y)^{1-3}$	3.1775(303)	$C_{yK}^{1-3} \times 10^3$	-0.41559(669)	$C_{yJ}^{1-3} \times 10^3$	-0.28308(128)
$C_{yKK}^{1-3} \times 10^6$	-0.5540(219)	$C_{yJK}^{1-3} \times 10^6$	1.5522(199)	$C_{yKKK}^{1-3} \times 10^9$	1.5088(457)
$C_{xz}^{1-3} \times 10$	0.24131(568)	$C_{xzK}^{1-3} \times 10^4$	-0.04933(207)	$C_{xzJ}^{1-3} \times 10^4$	0.22143(711)
$C_{xxKK}^{1-3} \times 10^7$	0.09681(775)	$C_{xxJK}^{1-3} \times 10^7$	0.2484(127)	$C_{xxJJ}^{1-3} \times 10^7$	-0.8873(167)
$C_{zK}^{1-3} \times 10^3$	0.6237(136)				
$(2A\zeta^z)^{2-3}$	3.0321(538)	$C_{zK}^{2-3} \times 10^3$	-0.19381(332)	$C_{zJ}^{2-3} \times 10^3$	0.12408(302)
$C_{zKK}^{2-3} \times 10^6$	0.7019(163)	$C_{zJJ}^{1-3} \times 10^6$	-0.5559(156)	$C_{zKKK}^{2-3} \times 10^9$	-0.1659(140)
$C_{xy}^{2-3} \times 10$	0.10904(102)	$C_{xyK}^{2-3} \times 10^4$	0.37018(590)	$C_{xyJ}^{2-3} \times 10^4$	-0.38761(576)
$C_{xyKK}^{2-3} \times 10^7$	0.4596(226)	$C_{xyJK}^{2-3} \times 10^7$	-1.4029(248)	$C_{xyJJ}^{2-3} \times 10^7$	0.52239(837)
$C_{yK}^{2-3} \times 10^3$	-1.0444(350)	$C_{yJ}^{2-3} \times 10^3$	0.35368(580)	$C_{yKK}^{2-3} \times 10^6$	-2.966(128)
$C_{yJK}^{2-3} \times 10^6$	2.210(124)	$C_{xxK}^{2-3} \times 10^4$	0.09313(512)	$C_{xxJ}^{2-3} \times 10^4$	-0.7781(108)
		$C_{xxKK}^{2-3} \times 10^7$	0.4286(106)		
Fermi-type interactions					
Parameter	Value	Parameter	Value	Parameter	Value
$F_0^{1-2}$	-14.263(486)	$F_K^{1-2} \times 10^2$	-4.5818(580)	$F_J^{1-2} \times 10^2$	2.7365(294)
$F_{KK}^{1-2} \times 10^4$	0.7260(118)	$F_{JK}^{1-2} \times 10^4$	-0.5618(107)	$F_{KKK}^{1-2} \times 10^7$	-0.93111(699)
$F_{KJJ}^{1-2} \times 10^7$	1.081(706)	$F_{xy}^{1-2} \times 10^2$	4.4567(203)	$F_{xyK}^{1-2} \times 10^4$	0.20449(615)
$F_{xyJ}^{1-2} \times 10^4$	0.03248(176)	$F_{xyKK}^{1-2} \times 10^6$	-0.03519(236)	$F_{xyJK}^{1-2} \times 10^6$	-0.11845(209)

<sup>a</sup> See footnote to Table 4.

5 ( $\nu_3$ ), and 8 ( $\nu_6$ ) together with their experimental uncertainties  $\Delta$  (columns 3, 6, and 9, respectively). It should be said that really the number of assigned transitions was a little bit larger than it is mentioned above. However, we used in the fit only the upper energies determined from the doubtlessly assigned lines.

It has been noted in the previous study (10) of the  $\nu_3$ ,  $\nu_4$ , and  $\nu_6$  triad that, owing to correlation effects, the fit was unstable,

rotational and Coriolis constants drastically changing, the latter also being dependent on the chosen reduction (10). In order to circumvent correlation problems we chose a different approach. Based on the experience that centrifugal distortion constants of excited states should be close to the ground state values we varied in the first step of our data fit only the band centers and the rotational constants. The centrifugal distortion constants were constrained to their ground state values. At the same time many

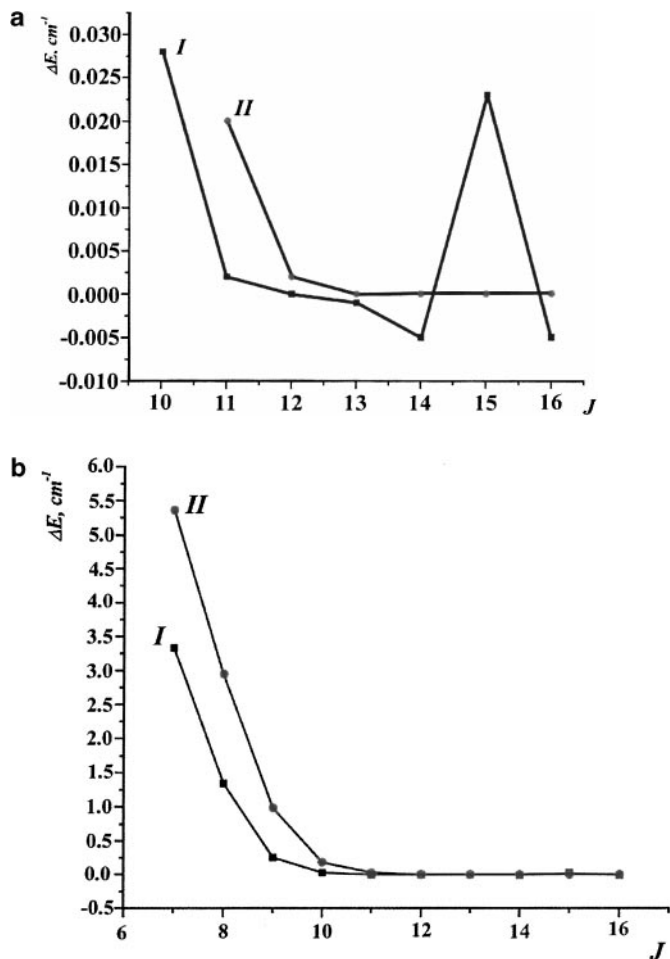


**FIG. 5.** Diagram of the dependence of the value  $\Delta J = E_{JK_a=6 K_c=J-6} - E_{JK_a=7 K_c=J-6}$  on the value of the quantum number  $J$ . Trace I corresponds to the vibrational state ( $v_4 = 1$ ). In this case, (a) shows in more detail the part of the general diagram; (b) concerns high values of the quantum number  $J$ . The unusual behavior of trace I is caused by the presence of strong resonance interactions of the states  $[JK_a = 6 K_c = J - 6](v_6 = 1)$  and  $[JK_a = 7 K_c = J - 6](v_4 = 1)$  with different states  $[JK_a K_c](v_4 = 1)$ . For comparison, diagram II shows the usual behavior of the value  $\Delta J = E_{JK_a=6 K_c=J-6} - E_{JK_a=7 K_c=J-6}$  versus the value of the quantum number  $J$  for the ground vibrational state.

interaction parameters were refined. This was compulsory because resonance interactions are numerous and strong. One such resonance interaction is illustrated in Fig. 5 where for the  $v_4 = 1$  (trace I) and the ground state (trace II) the energy difference  $\Delta J = E_{JK_a=6 K_c=J-6} - E_{JK_a=7 K_c=J-6}$  is displayed for different  $J$ .

One more strong resonance interaction that became detectable thanks to the superior resolution of the present spectra is the splitting of the energy cluster  $[J = 18 K_a = 18 K_c = 1]/[J = 18 K_a = 18 K_c = 0]$  of the vibrational state  $v_3 = 1$ . Table 6 illustrates that the clusters  $[JK_a = JK_c = 1]/[JK_a = JK_c = 0]$  ( $v_3 = 1$ ), both with the smaller and larger quantum numbers  $J$ , are unsplit while the  $J = 18$  cluster is split because of its strong interaction with the  $[J = 18 K_a = 13 K_c = 5]/[J = 18 K_a = 13 K_c = 6]$  ( $v_6 = 1$ ) states. The corresponding doublet

at 1113.41342 and 1113.42220  $\text{cm}^{-1}$  is found in the  $Q$  branch of the  $\nu_3$  band, and both transition wavenumbers are correctly predicted by our model. This doublet was not resolved in Ref. (10).

In the final step the centrifugal distortion constants  $\Delta_K$ ,  $\Delta_{JK}$ , and  $\Delta_J$  were also refined while all other centrifugal distortion constants up to octic terms were constrained to their ground state values. The excited state molecular parameters for the triad are reported in Table 4 and the interaction constants are given in Table 7. Altogether 21 molecular parameters and 50 interaction constants, in total 71 parameters, were refined. This may be compared with  $36 + 24 = 60$  and  $35 + 20 = 55$  parameters in sets 1 and 2 of Ref. (10). The larger number of parameters needed in the present study is required, above all, by the higher quantum numbers of the probed energy levels and the higher precision of the data. This latter criterium can be assessed by the  $\delta$  values given in columns 4, 7, and 10 of Table 6, which quote the differences in units of  $10^{-5} \text{ cm}^{-1}$  between experimental energies and those calculated with the parameters of Tables 4 and 7.

The Coriolis interaction constants and the rotational–vibrational constants  $\alpha_\lambda^{\beta}$  ( $\beta = x, y, z$  and  $\lambda = 3, 4$ , and 6) shown in column 3 of Table 3 may be compared with the predictions outlined in Section 2. Most of them are in reasonable agreement. This agreement is particularly noteworthy in view of the fact that PH<sub>3</sub> is not a “true local mode” molecule, the equilibrium interbond angle being near  $93.5^\circ$  rather than  $90^\circ$ , and the  $m_H/M_P$  ratio is close to  $1/31$ .

A further criterion for the physical significance of our model is the closeness of the final, refined excited state quartic centrifugal distortion constants  $\Delta_K$ ,  $\Delta_{JK}$ , and  $\Delta_J$  with regard to those of the ground state. While our  $\Delta$  difference values are on average 1.9% in absolute value and do not exceed 3.9%, the average/maximum  $D$  differences in Ref. (10) are much larger both in Model 1 and Model 2: 9.5/23.2 and 18.9/27.2%, respectively. The averaged absolute values of the  $D$  constants are about the same in Ref. (10) as the  $\Delta$  values in the present study in spite of the different representation used. Also the excited state  $d_1$  and  $d_2$  values in Model 2 (10) differ substantially from the ground state values.

## 6. CONCLUSION

For  $^M X^m Y_3$ ,  $C_{3v}$  symmetry molecules satisfying the above-mentioned local mode conditions, isotopic relations for the rotation–vibration  $\alpha_\lambda^{\beta}$ , and quartic centrifugal distortion parameters were derived for the case where one of the light atoms  $Y$  is replaced (here H by D). Our results were successfully tested for the assignment and the fit of a new high-resolution Fourier transform spectrum of PH<sub>2</sub>D in the region of the three lowest vibrational–rotational bands  $\nu_4$ ,  $\nu_6$ , and  $\nu_3$ . The analysis benefited from the precise, improved rotational energies of the ground vibrational state. This fact, on the one hand, and the higher resolution and higher sensitivity than in an earlier contribution (10) on the other hand, enabled us to assign transitions with higher values of quantum number  $J$  and to achieve higher accuracy in the values of rotation–vibration energies in the upper states

than in the earlier study. The fit of the obtained upper state energies in the framework of Watson's A-reduced Hamiltonian in  $\Pi^I$  representation leads to a physically meaningful set of 71 spectroscopic parameters which reproduce the 881 observed "experimental" energies with accuracies close to the experimental precision. It is to be expected that our approach to predicting parameters of isotopically substituted "daughter" species from those of the "mother" molecule will likewise be successful for other vibrations of  $\text{PH}_2\text{D}$ . Supposedly this method will be even more powerful if the target molecules fulfill local mode conditions better than  $\text{PH}_3$  and  $\text{PH}_2\text{D}$ , as is the case for  $\text{H}_2\text{Se}$  and  $\text{HDSe}$ , which were studied earlier (1, 2).

### ACKNOWLEDGMENTS

We thank the Deutsche Forschungsgemeinschaft and the Ministry of Education of the Russian Federation for financial support.

### REFERENCES

1. O. N. Ulenikov, G. A. Onopenko, N. E. Tyabaeva, H. Bürger, and W. Jerzembeck, *J. Mol. Spectrosc.* **197**, 100–113 (1999).
2. O. N. Ulenikov, G. A. Onopenko, N. E. Tyabaeva, H. Bürger, and W. Jerzembeck, *J. Mol. Spectrosc.* **198**, 27–39 (1999).
3. A. T. Tokunaga, R. F. Knacke, S. T. Ridgway, and L. Wallace, *Astrophys. J.* **232**, 603–615 (1979).
4. R. F. Knacke, S. J. Kim, S. T. Ridgway, and A. T. Tokunaga, *Astrophys. J.* **262**, 388–395 (1982).
5. L.-M. Lara, B. Bezard, C. A. Griffith, J. H. Lacy, and T. Owen, *Icarus* **131**, 317–333 (1988).
6. G. Tarrago, M. Dang-Nhu, and A. Goldstein, *J. Mol. Spectrosc.* **88**, 311–322 (1981).
7. D. Papoušek, H. Birk, U. Magg, and H. Jones, *J. Mol. Spectrosc.* **135**, 105–118 (1989).
8. A. Ainetschian, U. Häring, G. Spiegl, and W. A. Kreiner, *J. Mol. Spectrosc.* **181**, 99–107 (1996).
9. R. J. Kshirsagar and V. A. Job, *J. Mol. Spectrosc.* **161**, 170–185 (1993).
10. R. J. Kshirsagar and V. A. Job, *J. Mol. Spectrosc.* **185**, 272–281 (1997).
11. O. N. Ulenikov, H. Bürger, W. Jerzembeck, G. A. Onopenko, E. S. Bekhtereva, and O. L. Petrunina, *J. Mol. Struct.*, in press.
12. A. D. Bykov, Yu. S. Makushkin, and O. N. Ulenikov, *J. Mol. Spectrosc.* **85**, 462–479 (1981).
13. H. H. Nielsen, *Rev. Mod. Phys.* **23**, 90–135 (1951).
14. D. Papousek and M. R. Aliev, "Molecular Vibrational–Rotational Spectra," Elsevier, Amsterdam/Oxford/New York, 1982.
15. O. N. Ulenikov, R. N. Tolchenov, and Qing-shi Zhu, *Spectrochim. Acta Part A* **53**, 845–853 (1997).
16. G. M. McRae, M. C. L. Gerry, and E. A. Cohen, *J. Mol. Spectrosc.* **116**, 58–70 (1986).
17. K. Kijima and T. Tanaka, *J. Mol. Spectrosc.* **89**, 62–75 (1981).
18. G. Guelachvili and K. Narahari Rao, "Handbook of Infrared Standards," Academic Press, New York, 1986.